Supersonic Flow over a Rearward Facing Step with Transverse Nonreacting Hydrogen Injection

Harry A. Berman* and John D. Anderson Jr.†
University of Maryland, College Park, Maryland
and
J. Philip Drummond‡
NASA Langley Research Center, Hampton, Virginia

This work involves an application of computational fluid dynamics to a problem associated with the flow in the combustor region of a supersonic combustion ramjet engine (Scramjet). In particular, a time-dependent, finite difference method is used to solve the complete two-dimensional Reynolds averaged Navier-Stokes equations for the turbulent supersonic flow of air over a rearward-facing step, with transverse H_2 injection downstream of the step. To delineate the purely fluid dynamic effects, the flow is treated as nonreacting; however, detailed binary diffusion of H_2-air is included, along with a variable Lewis number. Results are obtained and compared for cases with and without H_2 injection. The influence of the wall temperature boundary conditions (adiabatic vs constant temperature) is studied, and is shown to have little impact on the flow both near and far away from the wall. These numerical results are the first to be obtained for this flow geometry, expecially at conditions germaine to a Scramjet. They demonstrate that such an application of computational fluid dynamics can be useful for the study of inlet-combustor interactions, and the flameholding potential of the rearward-facing step.

Nomenclature

a = speed of sound
c = Courant number
c_i = mass fraction
C_x, C_y = damping coefficients
D_{12} = diffusion coefficient, cm^2/s
h = height, static enthalpy
(i,j) = indexes for x and y directions, respectively
k = thermal conductivity
L = length
M = Mach number
p = pressure
Pr = Prandtl number
q = heat flux vector
R = specific gas constant
Re = Reynolds number
S = constant for Southerland's Law
t = time
T = temperature
u = x component of velocity
U = vector of dependent variables (ρ, ρu, ρv...)
v = y component of velcocity
V = velocity vector
V_i = diffusion velocity of species i
x,y = coordinate directions
y_i = mole fractions
γ = ratio of specific heats, c_p/c_v
δ = boundary-layer thickness
Δ = grid increment either x or y direction
η = local normal direction
μ = viscosity
ρ = density
τ = shear stress
Φ = viscous dissipation function
ω = vorticity

Subscripts and Superscripts

air = air
H_2 = hydrogen
L = length
le = local equilibrium
m = mixture
n = time level
t = turbulent
te = trailing edge
w = wall
x = mixture
∞ = freestream

Presented as Paper 82-1002 at the AIAA/ASME 3rd Joint Thermophysics, Fluid, Plasma and Heat Transfer Conference, St. Louis, Mo., June 7-11, 1982; submitted June 17, 1982; revision received March 14, 1983.

*Research Assistant, Department of Aerospace Engineering; presently Aerospace Engineer, David Taylor Naval Ship Research & Development Center. Member AIAA.
†Professor, Department of Aerospace Engineering. Associate Fellow AIAA.
‡Aerospace Engineer, Computational Methods Branch. Member AIAA.

I. Introduction

THIS work is an application of computational fluid dynamics to a problem associated with the flow in the combustor region of a supersonic combustion ramjet engine (scramjet). An airframe-integrated scramjet currently is being investigated at the NASA Langley Research Center.[1] The design concept is shown in Fig. 1. The engine is composed of several individual engine modules on the bottom surface of a hypersonic airframe (upper right of Fig. 1). Initial compression for the engine is performed by the vehicle forebody. Compression continues in the fixed geometry engine module inlet. Primary nozzle expansion is accomplished by careful contouring of the airframe at the engine exit. This scramjet propulsion concept becomes attractive over the speed regime of Mach 4-6.

Focusing on the combustor region shown in Fig. 1, three centrally located struts provide points from which hydrogen fuel is injected. Fuel is injected both tangential and per-

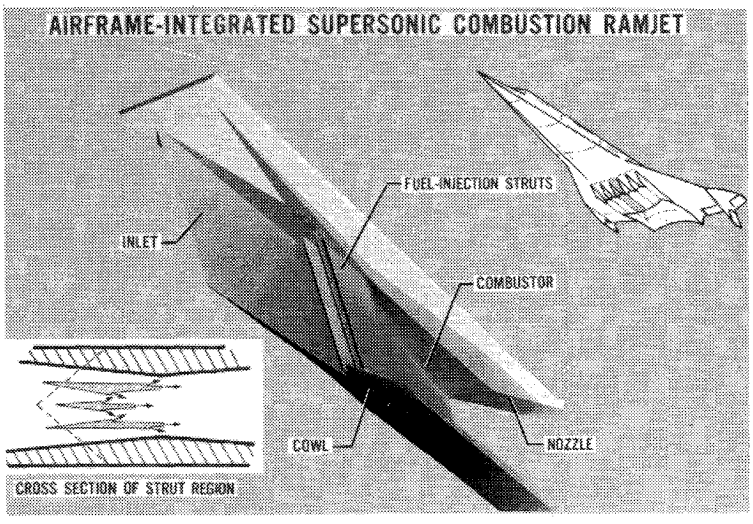

Fig. 1 Engine module and strut region cross section.

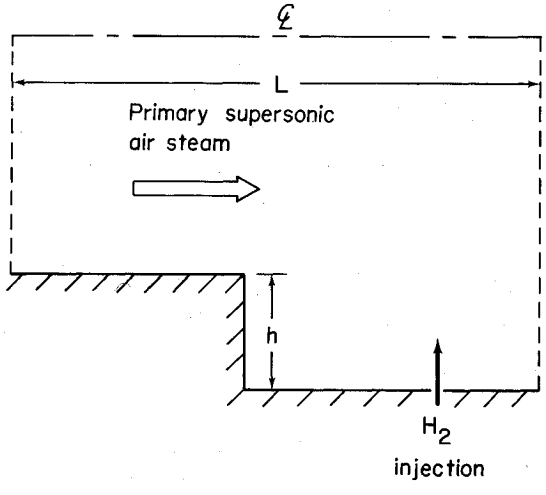

Fig. 2 Rearward facing step; computational domain.

pendicular to the prevailing flow direction. The speed regime over which the engine will operate necessitates the two modes of injection. At high speeds, the perpendicular injection dominates; this facilitates mixing and aides in localizing the combustion process in the immediate area of the combustor struts. On the other hand, at lower speeds, such perpendicular injection may cause too rapid mixing and combustion, hence thermally choking the flow. Therefore, tangential injection is used at lower speeds to spread out the combustion region.

Examining the sketch at the bottom of Fig. 1, the flow in the vicinity of some of the fuel injection ports is characterized by supersonic flow over a rearward-facing step, with transverse H_2 injection downstream of the step. This physical problem, sketched in Fig. 2, is the subject of the present paper. The flowfield is dominated by regions of separated flow, and by mixed regions of locally subsonic and supersonic flow. The objective of this work is to solve numerically the flowfield in the vicinity of the rearward-facing step and the H_2 injection port, and to study its fluid dynamic aspects. Indeed, in order to isolate some of the purely fluid dynamic phenomena, the H_2 is not allowed to chemically react with the primary air stream; rather, the problem treats a binary nonreacting gas. Such a model sheds light on how the fluid dynamics affects the viability of the rearward-facing step geometry as a flameholder and as a mechanism to isolate the inlet from the combustor.

In addition to the preceding, the present paper addresses the following question. How are the numerical flowfield results affected by the wall temperature boundary condition, i.e., what is the effect of constant wall temperature vs adiabatic wall boundary conditions? Since the practical design of a scramjet engine must account for severe heat transfer problems, such a question is important for numerical calculations of scramjet flows. The present paper discusses a series of numerical experiments designed to study this question.

This work represents the first detailed numerical calculations of the rearward-facing step/H_2 injection flowfield germaine to scramjet combustors. Moreover, it is the first to study the influence of different wall temperature boundary conditions for such geometry. This work should be of interest to other investigators dealing with the numerical solutions of general, viscous, mixed subsonic-supersonic, separated flows.

This work is a natural complement to the previous calculations of Drummond et al.,[2-4] which treated the case of transverse H_2 injection into a supersonic air stream over a flat surface. In Refs. 2-4, the two-dimensional Navier-Stokes equations are solved by means of a time-dependent finite difference method, with an algebraic eddy viscosity model used to simulate the effects of turbulence. The present paper is an extension of Drummond's work to the case of a rearward-facing step, with H_2 injection downstream of the step.

Referring again to the fuel injection struts shown in Fig. 1, note that H_2 also is injected tangentially to the primary flow at the base region of the struts. The numerical study of such base flow with injection is given in a companion paper by Sullins et al.[5]

II. Governing Equations

Navier-Stokes Equations

The flowfield to be analyzed, Fig. 2, is governed by the complete compressible form of the Navier-Stokes equations, neglecting body forces and heat source terms, along with global and species continuity equations and an energy equation.[6,7] Also, a two-equation algebraic turbulence model is utilized.

In conservation form, the governing equations are as follows.

Continuity:

$$\frac{\partial \rho}{\partial t} + \nabla \cdot (\rho V) = 0 \tag{1}$$

Species Continuity:

$$\frac{\partial (\rho c_i)}{\partial t} = -\nabla \cdot [\rho c_i (V + V_i)] \tag{2}$$

x Momentum:

$$\frac{\partial(\rho u)}{\partial t}+\nabla\cdot(\rho uV)=-\frac{\partial p}{\partial x}+\frac{\partial}{\partial x}\left[\mu\left(2\frac{\partial u}{\partial x}-\frac{2}{3}\nabla\cdot V\right)\right]+\frac{\partial}{\partial y}\left[\mu\left(\frac{\partial u}{\partial y}+\frac{\partial v}{\partial x}\right)\right] \tag{3}$$

y Momentum:

$$\frac{\partial(\rho v)}{\partial t}+\nabla\cdot(\rho vV)=-\frac{\partial p}{\partial y}+\frac{\partial}{\partial y}\left[\mu\left(2\frac{\partial v}{\partial y}-\frac{2}{3}\nabla\cdot V\right)\right]+\frac{\partial}{\partial x}\left[\mu\left(\frac{\partial u}{\partial y}+\frac{\partial v}{\partial x}\right)\right] \tag{4}$$

Energy:

$$\frac{\partial(\rho h)}{\partial t}+\nabla\cdot(\rho hV)=-\nabla\cdot q+\frac{Dp}{Dt}+\mu\Phi-\nabla\cdot(\Sigma\rho_i V_i h_i) \tag{5}$$

Equation of state:

$$p=\rho RT \tag{6}$$

Molecular Viscosity Calculation

The molecular viscosity $\bar{\mu}$ is calculated using Southerland's law with appropriate constants for each species calculated[8]

$$\frac{\bar{\mu}}{\bar{\mu}_\infty}=\left(\frac{T}{T_\infty}\right)^{3/2}\frac{T_\infty+S}{T+S} \tag{7}$$

where $\bar{\mu}_\infty$ and T_∞ are reference values. This formula is applicable for single component gases only. For the cases of interest in which hydrogen and air are present. Wilke's formulation was used to calculate the mixture viscosities.[9]

For a binary gas, Wilke's formula is

$$\bar{\mu}_m=\bar{\mu}_1/[1+y_2/y_1\phi_{12}]+\bar{\mu}_2/[1+y_1/y_2\phi_{21}] \tag{8}$$

where y_1 and y_2 are mole fractions, and

$$\phi_{12}=[1+(\bar{\mu}_1/\bar{\mu}_2)(M_2/M_1)^{1/4}]^2/[\sqrt{8}(1+M_1/M_2)^{1/2}] \tag{9}$$

$$\phi_{21}=\phi_{12}(\bar{\mu}_2/\bar{\mu}_1)(M_1/M_2) \tag{10}$$

These formulas allow for the calculation of the mixture viscosities relying only on the individual viscosity components, the mole fractions, and the molecular weights.

Molecular Thermal Conductivity

The molecular thermal conductivity $\bar{k}$ is calculated using Southerland's law with the appropriate constants.[8]

$$\frac{\bar{k}}{\bar{k}_\infty}=\left(\frac{T}{T_\infty}\right)^{3/2}\frac{T_\infty+S}{T+S} \tag{11}$$

An equation attributed to Wassiljewa for the thermal conductivity is used when multicomponent gases are present.

$$\bar{k}_m=\bar{k}_1/[1+A_{ij}(y_2/y_1)]+\bar{k}_2/[1+A_{ji}(y_1/h_2)] \tag{12}$$

When A_{ij} is replaced by

$$A_{ij}=1.065\phi_{ij} \tag{13}$$

this formulation differs from Wilke's formula for mixture viscosities only by a constant.

Molecular Diffusion

Diffusion is treated by means of Fick's law

$$\rho_i V_i=-\rho\bar{D}_{12}\nabla c_i \tag{14}$$

An expression for the molecular binary diffusion coefficient $\bar{D}_{12}$ is obtained from kinetic theory for dilute gases[10]

$$\bar{D}_{12}=\frac{0.001858T^{3/2}((M_1+M_2)/M_1M_2)^{1/2}}{p\sigma_{12}^2\Omega_D} \tag{15}$$

An expression for the collision integral is given by White[8] to be

$$\Omega_D\approx T^{*-0.145}+(T^*+0.05)^{-2} \tag{16}$$

$$T^*=T/T_{\epsilon_{12}} \tag{17}$$

$$T_{\epsilon_{12}}=(T_{\epsilon_1}T_{\epsilon_2})^{1/2} \tag{18}$$

The effective collision diameter is determined by

$$\sigma_{12}=\tfrac{1}{2}(\sigma_1+\sigma_2) \tag{19}$$

Values for T_{ϵ_1}, T_{ϵ_2}, σ_1, and σ_2 are taken from White.[8] Equations (15-19) yield the necessary information to apply Fick's law [Eq. (14)].

Turbulence Model

The rearward facing step geometry produces a highly turbulent flowfield at the Mach numbers and Reynolds numbers considered in this investigation. Two primary flowfield phenomena are present in this investigation: recirculation regions and a strong shock/expansion region in the vicinity of the injection port. The inclusion of these phenomena in the flowfield led to the decision to use an algebraic model developed by Baldwin and Lomax.[11] The primary advantage of this model is that the boundary-layer thickness does not need to be calculated; rather, the model is based upon the local vorticity ω. This particularly is helpful since in the region of the injection port, the boundary-layer thickness is difficult to define. Reference 11 gives a two-layer algebraic eddy viscosity model which defines μ_t as

$$\begin{aligned}\mu_t&=(\mu_t)_{\text{inner}} \qquad y\le y_{\text{crossover}}\\ &=(\mu_t)_{\text{outer}} \qquad y\ge y_{\text{crossover}}\end{aligned} \tag{20}$$

where y is the local normal distance from a solid surface. The crossover point in y is the point at which $(\mu_t)_{\text{outer}}$ becomes less than $(\mu_t)_{\text{inner}}$.

The value of viscosity in the inner region is given by the formula

$$(\mu_t)_{\text{inner}}=\rho\ell^2|\omega| \tag{21}$$

where

$$\ell=ky[1-\exp(-y^+/A^+)] \tag{22}$$

$$y^+=\sqrt{\rho_w\tau_w}y/\mu_w \tag{23}$$

The vorticity ω is defined for two-dimensional flow as

$$|\omega|=\sqrt{\left(\frac{\partial u}{\partial y}-\frac{\partial v}{\partial x}\right)^2} \tag{24}$$

For the outer region

$$(\mu_t)_{\text{outer}}=KC_{\text{cp}}F_{\text{wake}}F_{\text{kleb}} \tag{25}$$

F_{wake} is taken to be the minimum of $Y_{\max}F_{\max}$ or $C_{\text{wake}}Y_{\max}U^2_{\text{dif}}/F_{\max}$. $Y_{\max}$ is the y distance at which $F_{\max}$ occurs with $F_{\max}$ being the maximum value of $F(y)$ in a given transverse profile. The function $F(y)$ is given by

$$F(y)=y|\omega|(1-\exp(-y^+/A^+)) \tag{26}$$

The value of U_{dif} is found by taking the difference between the maximum and minimum velocities in a given profile;

however, $(U_{dif})_{min}$ equals zero everywhere. Therefore,

$$U_{dif} = \sqrt{u^2 + v^2} \tag{27}$$

The value of F_{kleb}, the Klebanoff intermittency factor, is given by

$$F_{kleb}(y) = \left[1 + 5.5\left(\frac{C_{kleb}\, y}{Y_{max}}\right)^6\right]^{-1} \tag{28}$$

The six constants necessary for this model are: $A^+ = 26.0$, $C_{cp} = 1.6$, $C_{kleb} = 0.3$, $C_{wake} = 0.25$, $k = 0.4$, and $K = 0.0168$. These constants are taken directly from Ref. 11 with the understanding that, while they are not precisely the correct constants for this flowfield geometry, they have been used successfully in examining similar types of flowfields.[2-4]

This model uses the normal distance form the wall as a primary variable in determining the turbulent viscosity. For the rearward facing step problem, an ambiguity arises in considering this geometry since there is a discontinuity in the normal direction. This discontinuity in y leads to a discontinuous jump in the viscosity values in the area of the step. In order to smooth this discontinuity, a relaxation equation is used as given by Waskiewicz et al.[12]

$$\frac{\mu_t - \mu_{te}}{\mu_{le} - \mu_{te}} = 1 - \exp\left(-\frac{\Delta x}{\lambda \delta_{te}}\right) \qquad x > x_{te} \tag{29}$$

This proved to be very satisfactory in smoothing out the discontinuity. The value of viscosity μ in the governing equations is now equal to

$$\mu = \bar{\mu} + \mu_t \tag{30}$$

The values of the turbulent thermal conductivity k_t and diffusion coefficient D_t were obtained from μ_t by assuming a constant turbulent Prandtl and Lewis number equal to 0.91 and 1.0, respectively.

$$\mu_t C_p / k_t = 0.91 \qquad \rho D_t C_p / k_t = 1.0$$

The final values of k and D_{12} in the governing equations are

$$k = \bar{k} + k_t \tag{31}$$

and

$$D_{12} = \bar{D}_{12} + D_t \tag{32}$$

III. Numerical Technique

The present numerical solution of Eqs. (1-6) is patterned after the explicit, time-dependent, unsplit, predictor-corrector, finite difference method given by MacCormack in 1969.[13] MacCormack's explicit method is well-known, and has become a popular technique for the numerical solution of a wide variety of fluid dynamic problems over the past decade. This time-dependent method is described in detail in Chap. 12 of Ref. 6, and its application to the present problem is discussed at length in Ref. 14. Therefore, no further details of the finite difference solution will be given here.

During the course of the present numerical solutions, it was found necessary to add some artificial viscosity to the equations in order to damp numerical oscillations induced by the severe transient gradients in the flowfield associated with the rearward-facing step. The fourth-order damping term introduced by Holst[15] was used in the present set of equations. The details are presented in Ref. 14.

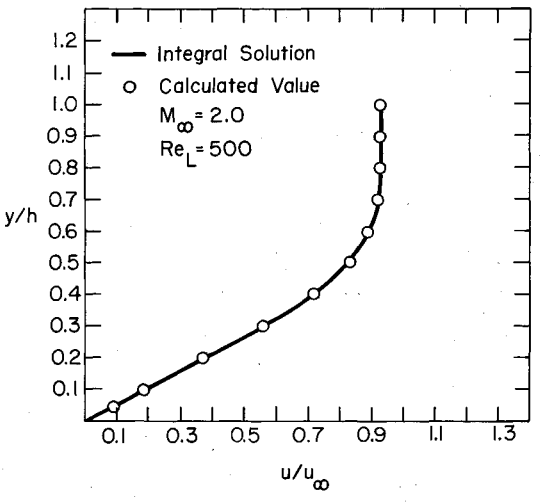

Fig. 3 Velocity profile; flat plate.

Boundary Conditions

Along the supersonic inflow boundary all values are held fixed with respect to time. Along the wall the no slip condition is enforced along with the condition that the normal pressure gradient vanishes at the wall.

$$u = 0, \qquad v = 0, \qquad \partial p / \partial n = 0 \tag{33}$$

The value of the dependent variables along the top boundary were found either by extrapolation based on the method of characteristics, or the top boundary was treated as a symmetry plane (hydrogen injection cases).

The supersonic outflow boundary values were found by linear extrapolation from the interior points.

Convergence Criteria

A convergence criteria was developed based on examination of the transient flowfield. It has been found that, in general, the last flowfield variable to converge is the density, therefore, the following convergence criteria was established:

$$A = \frac{\rho_{old} - \rho_{new}}{\rho_{ols}} \text{ where } A \leq 0.0005 \tag{34}$$

at every point in the flowfield from one time step to the next.

IV. Results and Discussion

In this section, Navier-Stokes solutions are presented for the supersonic flow over a rearward-facing step with and without H_2 injection. However, to establish the integrity of the computer program (written by the lead author), two simpler test cases were calculated: 1) supersonic laminar flow over a flat plate, where comparisons are made with a previous, standard, integral boundary-layer solution; and 2) hypersonic laminar, low Reynolds number flow over a rearward-facing step, where comparisons are made with existing data. These test cases are discussed first, and then are followed by the present results for supersonic, turbulent flow over a rearward-facing step with and without H_2 injection.

Flat Plate

In order to ascertain whether the basic programming of the Navier-Stokes equations was correct, the present computer code was applied to the supersonic laminar flow over a flat plate. The test conditions were $M_\infty = 2.0$, $Re_L = 500$, $T_w/T_\infty = 2.0$. A comparison between the present Navier-Stokes numerical results and an integral solution given by Allen and Cheng[16] is shown in Fig. 3; excellent agreement is obtained.

Laminar Test Case

In Ref. 17, numerous experimental results are given for the hypersonic, laminar, low Reynolds number flow over a rearward-facing step. Of these, the specific case chosen for comparison with the present numerical results is the 0.51-cm step with $T_t = 3750$ K and $p_t = 1.605$ atm. The experimental

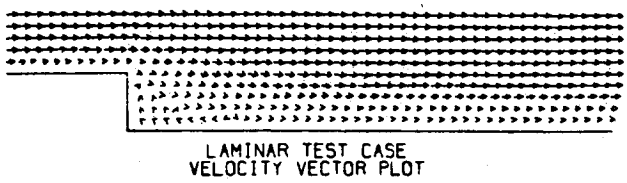

Fig. 4 Computed velocity field for the experimental conditions given in Ref. 17; 6157 time steps, converged solution.

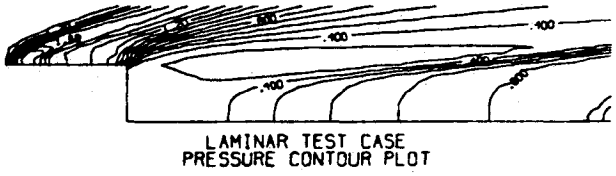

Fig. 5 Computed pressure field for the experimental conditions given in Ref. 17, 6157 time steps, converged solution.

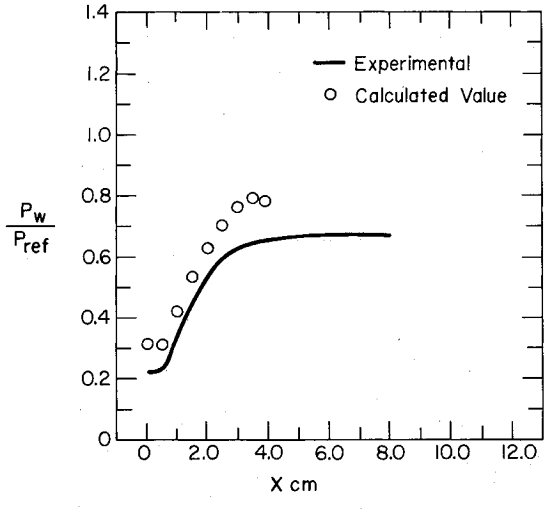

Fig. 6 Laminar test case; surface pressure distribution downstream of step. Experimental data are taken from Ref. 17.

data were obtained in a high-temperature, arc-driven hypersonic wind tunnel. The partially dissociated air in the experiments is simulated by a frozen flow with $\gamma = 1.31$, $T_\infty = 1046$ K, and $p_\infty = 744$ N/m^2. Figures 4 and 5 illustrate the predominant flowfield characteristics. The velocity vector plot clearly shows the recirculation region directly behind the step, including the reattachment point. The pressure contour plot p/p_∞, given in Fig. 5, clearly shows the expansion fan at the corner, and the recompression region which begins in the area of the reattachment point. The recirculation region is also seen to be an area of nearly constant pressure. In Fig. 6, a direct comparison with the experimental data is made. Figure 6 is a plot of nondimensional wall pressure vs distance downstream of the step. As can be seen, the calculated trends agree with the experimental data; however, there are quantitative differences of as much as 25%. The differences in the wall pressures may be partly due to the fact that the gas mixture in the experiment was not standard air but a dissociated mixture which could not be accounted for adequately in the present computer code. Even though the numerical results do not match exactly with the experimental results, the code does correctly predict the resolve the predominant flowfield features, and, in conjunction with the flat plate comparison, a degree of confidence in the code has been established.

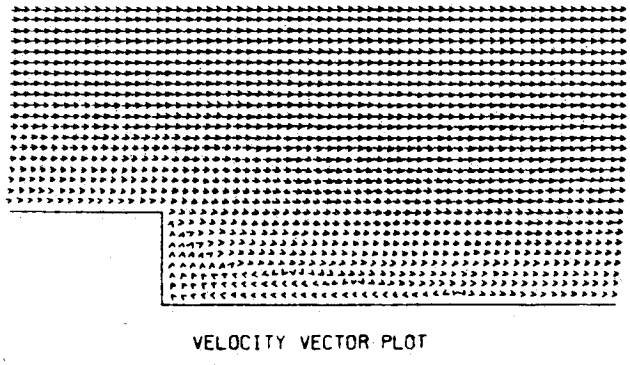

Fig. 7 Case without injection; 4447 time steps, converged solution.

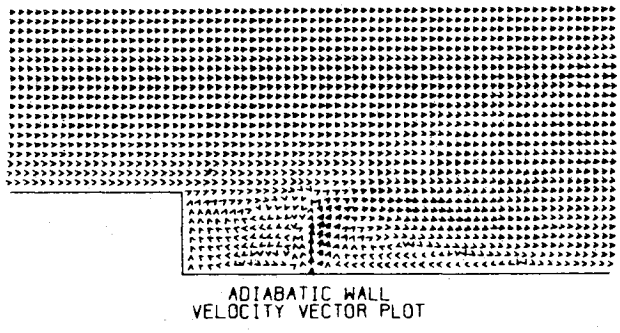

Fig. 8 Case with injection.

Case without Injection

The flow conditions for the hydrogen injection runs were chosen so as to simulate actual scramjet engine test conditions as close as was practically possible. An initial calculation was made without injection to further study the basic flowfield of the rearward facing step. The inflow conditions are taken from numerical work by Drummond.[2] Using Drummond's calculations for the full engine case, the step was taken to be at the point of minimum cross section for the engine. The reference values for this case are $M_\infty = 2.19$, $T_\infty = 1005.1$ K, $p_\infty = 120544$ N/m^2, $L = 3.5$ cm, $h = 0.5$ cm and $Re = 70{,}000$ (based on step height) (see Fig. 2 for the definition of L and h). For these conditions, the velocity vector plot in Fig. 7 shows the recirculation pattern with reattachment occurring approximately three step heights downstream of the step. The separation region becomes thin and elongated in the area of reattachment. A boundary-layer type of profile can be seen at the outflow station. In the recirculation region, the velocities are very low; the Mach numbers are on the order of 0.2. Other characteristics of this flow will be discussed in subsequent figures where comparison is made with the H_2 injection case.

Hydrogen Injection Case (Adiabatic Wall)

The flowfield shown in Fig. 7 is radically changed by the transverse injection of H_2. The case of sonic injection through a slot located 1.5 step height downstream of the step is illustrated in Fig. 8. The ratio of step height to injection slot width is 10:1. This velocity vector diagram corresponds to an adiabatic wall case; results for a constant temeprature wall will be discussed in a subsequent section. The conditions of the H_2 jet at the slot are $T_{jet}/T_\infty = 0.33$, $M_{jet} = 1.05$, and $p_{jet}/p_\infty = 3.033$. These conditions correspond to a fuel-air equivalence ratio of 0.25 for the scramjet. Also, note that the present two-dimensional calculations model injection through a slot, whereas in the actual engine, injection takes place through a series of orifices. Nevertheless, such a two-dimensional representation of the actual three-dimensional injection yields useful qualitative results for the analysis of engine flowfields.[2]

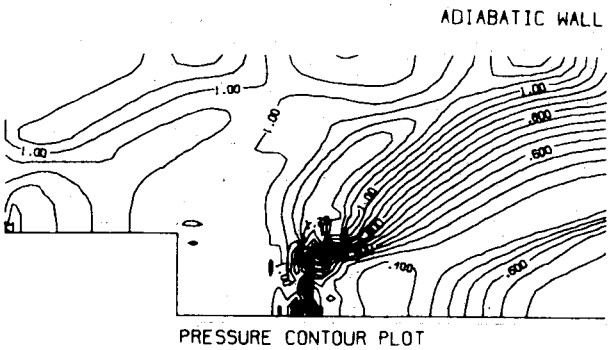

Fig. 9a Case with injection.

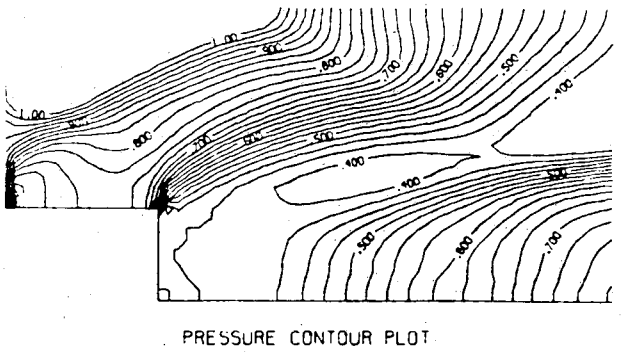

Fig. 9b Case without injection; 4447 time steps.

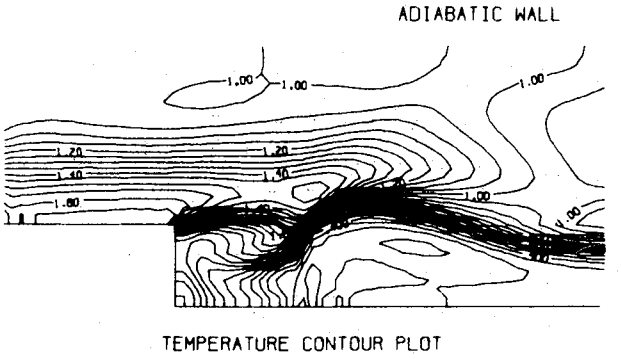

Fig. 10a Case with injection.

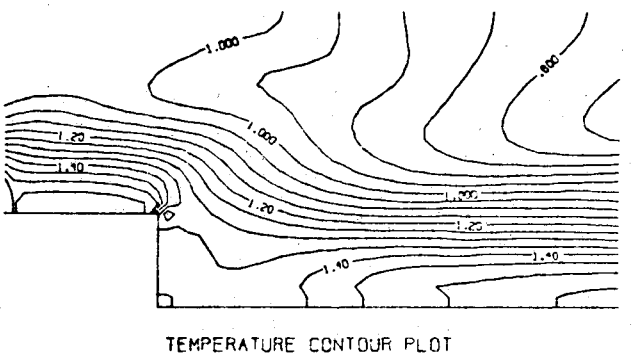

Fig. 10b Case without injection; 4447 time steps.

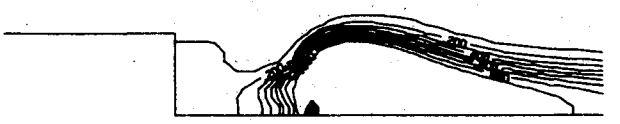

Fig. 11 H_2 mass fraction field, illustrating the extent of jet penetration and diffusion; constant temperature wall.

Comparing Fig. 8 (with injection) with Fig. 7 (without injection), the H_2 injection is seen to set up two primary regions of separated, recirculating flow, one between the step and the jet, and another downstream of the jet. In Fig. 8, the recirculation region between the step and the jet consists of two primary counter-rotating vortices; the vortex immediately adjacent to the step rotates in a clockwise direction (the same as the clockwise rotation seen in Fig., 7), whereas the vortex immediately upstream of the jet rotates in a counter-clockwise direction. The separated flow immediately downstream of the jet is rather elongated near the wall, and has a clockwise rotation. Note that the flow upstream of the step remains attached to the wall in spite of the presence of the jet. Hence, for the case treated here, the rearward-facing step is fulfilling one of its functions in a scramjet, namely, the isolation of the inlet from the combustor. Indeed, such results demonstrate the importance of detailed flowfield calculations to study the inlet-combustor interaction problem.

The two flowfields with and without injection are further compared in Fig. 9, which gives the pressure contours for the cases with injection (Fig. 9a) and without injection (Fig. 9b). Pressure contours are useful for visualizing expansion and compression waves in the flow. For example, examining Fig. 9b for no injection, the expansion wave from the corner and the recompression shock forming downstream of reattachment point are clearly seen. Also, Fig. 9b shows that the separated flow downstream of the step is an essentially constant pressure region, with an average base pressure of $p_{base}/p_\infty = 0.435$. However, when the H_2 is turned on, the nature of the flowfield changes completely. The H_2 jet is essentially acting as an effective body which masks the rearward-facing step from the primary flow; hence, the wave pattern in the primary flow is completely changed, as seen in Fig. 9a. Note that the expansion and compression waves seen in Fig. 9b are negated by the presence of the H_2 jet. Also note that injection increases the base pressure; $p_{base}/p_\infty = 0.996$ for the injection case.

The temperature contours with and without injection are compared in Figs. 10a and b, respectively. Temperature contours are useful in visualizing shear layers. A mixing layer is clearly seen at the top region of the H_2 jet in Fig. 10a.

Hydrogen Injection Case (Constant Temperature Wall)

The wall-temperature boundary condition has a relatively mild impact on the flowfield result for the case treated here. The previous case was repeated, except that the wall temperature boundary condition was changed to a constant wall temperature of 1000 K. This temperature is characteristic of actual experimental engine conditions.[18] The pertinent flowfield characteristics (jet penetration height, distribution of H_2, etc.) where found to be nearly identical for both wall-temperature boundary conditions. Contour plots for the constant temperature wall case are given in Ref. 19, which should be consulted for more details.

Figure 11 gives the H_2 mass fraction contours, and indicates that the recirculation region immediately downstream of the step is fuel rich, due to the combined effects of convection and mass diffusion. The H_2 mass fraction for stoichiometric conditions is about 0.03; the results in Fig. 11 indicate much higher values in the flameholding region.

V. Conclusions

1) This work represents the first, detailed numerical calculations of the supersonic flow over a rearward-facing step with transverse H_2 injection at conditions germaine to the combustor region of a scramjet engine.

2) The H_2 jet acts as an effective body which essentially shields the primary flow from the rearward-facing step, thus substantially changing the wave pattern in the primary flow.

3) For both cases with and without H_2 injection, the separated flow immediately downstream of the rearward-facing step is a region of essentially constant pressure at a low subsonic Mach number.

4) For both cases with and without injection, the flow is attached on the upper surface all the way to the corner of the step. Hence, for the case treated here, the rearward-facing step is serving its purpose of isolating the scramjet inlet from the combustor.

5) Through the combined mechanisms of diffusion and convection, enough H_2 makes its way upstream of the injection port to make the separated region between the step and the injector fuel rich. This has implications for the flameholding capability of such a flow.

6) For the case treated here, when the wall-temperature boundary condition is changed from an adiabatic wall to a constant temperature wall the flowfield is relatively unaffected.

7) The preceding results pertain to flow conditions chosen to simulate the flow in a scramjet combustor. The present analysis appears to be a useful tool in the study of such flows. Moreover, the results should be of general interest to investigators working in the over-all area of supersonic, viscous, separated flows.

VI. Acknowledgments

This work was performed under the support of NASA Grant NCC1-41, and is part of an ongoing program at the University of Maryland in the area of applications of computational fluid dynamics to practical engineering problems. The computer program used for these calculations was written completely by the lead author as part of his MS Thesis research at the University of Maryland.

References

[1] Jones, R. A. and Huber, P. W., "Toward Scramjet Aircraft," *Astronautics and Aeronautics*, Vol. 16, Feb. 1978, pp. 38-48.

[2] Drummond, J. P. and Weidner, E. H., "Numerical Study of a Scramjet Engine Flowfield," AIAA Paper 81-0186, Jan. 1981.

[3] Drummond, J. P., Rogers, R. C., and Evans, J. S., "Combustor Modeling for Scramjet Engines," AGARD 54th(B) Specialists' Meeting on Combustor Modeling, Propulsion and Energetics Panel, Cologne, Germany, Oct. 1979.

[4] Drummond, J. P., "Numerical Investigation of the Perpendicular Injector Flowfield in a Hydrogen Fueled Scramjet," AIAA Paper 79-1482, July 1979.

[5] Sullins, G. A., Anderson, J. D. Jr., and Drummond, J. P., "Numerical Investigation of Supersonic Base Flow with Parallel Injection," AIAA Paper 82-1001, 1982.

[6] Anderson, J. D., *Modern Compressible Flow: With Historical Perspective,* McGraw-Hill Book Co., New York, 1982.

[7] Schlichting, H., *Boundary Layer Theory*, McGraw-Hill Book Co., New York, 1979.

[8] White, F. M., *Viscous Fluid Flow,* McGraw-Hill Book Co., New York, 1974.

[9] Wilke, C. R., "A Viscosity Equation for Gas Mixtures," *Journal of Chemical Physics*, Vol. 18, No. 4, April 1950, pp.

[10] Reid, R. C. and Sherwood, T. K., *The Properties of Gases and Liquids-Their Estimation and Correlation*, McGraw-Hill Book Co., New York, 1966.

[11] Baldwin, B. S. and Lomax, H., "Thin Layer Approximations and Algebraic Model for Separated Turbulent Flows," AIAA Paper 78-257, 1978.

[12] Waskiewicz, J. D., Shang, J. S., and Hankey, W. L., "Numerical Simulation of Near Wakes Utilizing a Relaxation Turbulence Model," *AIAA Journal*, Vol. 18, Dec. 1980, pp. 1440-1445.

[13] MacCormack, R. W., "The Effect of Viscosity in Hypervelocity Impact Cratering," AIAA Paper 69-354, 1969.

[14] Berman, H. A., "A Numerical Solution of the Supersonic Flow Over a Rearward Facing Step with Transverse Hydrogen Injection," Masters Thesis, Dept. of Aerospace Engineering, Univ. of Maryland, College Park, Md., Oct. 1981.

[15] Holst, T. L., "Numerical Solution of Axisymmetric Boattail Fields with Plume Simulators," AIAA Paper 77-224, 1977.

[16] Allen, J. S. and Cheng, S. I., "Numerical Solutions of the Compressible Navier-Stokes Equations for the Laminar Near Wake," *Physics of Fluids*, Vol. 13, Jan. 1970, pp. 37-52.

[17] Jakubowski, A. K. and Lewis, C. H., "Experimental Study of Supersonic Laminar Base Flow with and without Suction," *AIAA Journal*, Vol. 11, Dec. 1973, pp. 1670-1677.

[18] Mackley, E., private communication, Hypersonic Propulsion Branch, NASA Langley Research Center, Hampton, Va., Dec. 1981.

[19] Berman, H. A., Anderson, J. D. Jr., and Drummond, J. P., "A Numerical Solution of the Supersonic Flow Over a Rearward Facing Step with Transverse Non-Reacting Hydrogen Injection," AIAA Paper 82-1002, 1982.